

## Increased frequency shifts in high aspect ratio terahertz split ring resonators

Sher-Yi Chiam,<sup>1</sup> Ranjan Singh,<sup>2</sup> Jianqiang Gu,<sup>2,3</sup> Jianguang Han,<sup>1</sup> Weili Zhang,<sup>2</sup> and Andrew A. Bettiol<sup>1,a)</sup>

<sup>1</sup>Department of Physics, National University of Singapore, 2 Science Drive 3, Singapore 117542, Singapore

<sup>2</sup>School of Electrical and Computer Engineering, Oklahoma State University, Stillwater, Oklahoma 74078, USA

<sup>3</sup>Key Laboratory of Opto-electronics Information and Technical Science (Ministry of Education), Center for Terahertz Waves and College of Precision Instrument and Optoelectronics Engineering, Tianjin University, Tianjin 300072, People's Republic of China

(Received 27 November 2008; accepted 19 January 2009; published online 9 February 2009)

The resonance of split ring resonators (SRRs) is known to shift upon the addition of a dielectric overlayer, a feature useful for practical applications. Here, we demonstrate that the frequency shift is enlarged by increasing the SRR height, thereby potentially enhancing sensitivity and tunability. We fabricated SRRs resonating at terahertz frequencies using a focused proton beam. This resulted in SRRs nearly 10  $\mu\text{m}$  high, with smooth and vertical sidewalls. Terahertz time domain spectroscopy was used for characterization. Upon applying a dielectric overlayer ( $\epsilon=2.7$ ), a resonance located at 640 GHz shifted by nearly 120 GHz. Simulations also indicate a widening frequency shift as SRR height increases. © 2009 American Institute of Physics.

[DOI: 10.1063/1.3079419]

There has been intense research on metamaterials in this decade, and recently there has been an increasing focus on practical applications for metamaterials. The terahertz regime is an active area for such research. For example, studies on the use of split ring resonators (SRRs) (Ref. 1) and frequency selective surfaces<sup>2,3</sup> for terahertz sensing of biological and chemical samples have been conducted. Metamaterials generally consist of resonant subwavelength metallic elements. Such sensing applications exploit the shift in the resonance frequency, which occurs when a dielectric sample—such as DNA—is deposited over a metamaterial surface. The shift is caused by the sample changing the electrical permittivity ( $\epsilon$ ) around the metamaterial. Using the same principle, Driscoll *et al.*<sup>4</sup> demonstrated passive frequency tuning with SRRs, where the resonance is shifted by the controlled application of silicon nanospheres. Frequency agile terahertz metamaterials have also been demonstrated by Chen *et al.*<sup>5</sup> Such frequency agility will allow the manufacturing of devices such as tunable notch filters.

It is clearly desirable that a sensing device is able to detect a small change in the dielectric environment. Improving sensitivity with metamaterial devices has been the subject of much research effort. For example, Debus and Bolivar<sup>2</sup> proposed the use of asymmetrical double split resonators (aDSRs), which have a very sharp edge in their frequency response thus allowing smaller changes in resonance frequency to be detected. Al-Naib *et al.*<sup>3</sup> further demonstrated increased volumetric sensitivity in aDSRs by adding sharp tips to the resonator arms thus intensifying the electric field in the resonator gaps. So far, conventional fabrication techniques—such as photolithography and sputtering—have been used to fabricate the metamaterials used for sensing and tunability demonstrations. Such techniques result in planar metamaterial elements of limited height. We thus explore

another way in which sensitivity can be improved—by increasing the height (aspect ratio) of the metamaterial elements. An increase in the height, for example, of SRRs would increase the high-field region in the SRR gap, raising the effective volume of the dielectric probed. There is, therefore, a clear interest in studying higher aspect ratio metamaterials.

In this paper, we fabricated high aspect ratio SRRs using a direct write technique called proton beam writing (PBW), which utilizes a focused MeV proton beam.<sup>6,7</sup> Due to their large mass relative to electrons, MeV protons will not significantly deviate from a straight line even as they travel through several tens of microns of resist. Although the proton beam generates secondary electrons, these remain very close to the incident-beam axis and proximity effects are very limited. We then demonstrate the ability of such high aspect ratio SRRs to achieve large shifts in their resonance frequency compared to their planar counterparts.

In the fabrication process, we first used PBW to write a latent image of the SRRs in (12  $\mu\text{m}$  thick) polymethylmethacrylate (PMMA) resist spin coated onto metalized silicon (Si) substrates. After development, an electroplating pro-

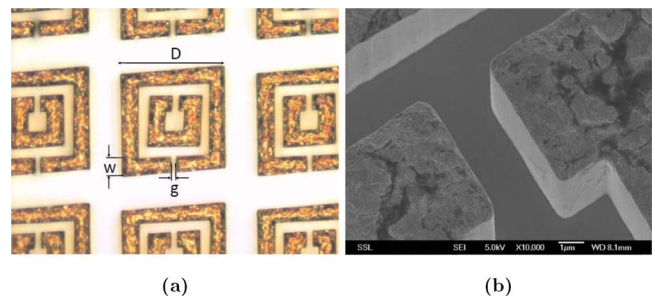


FIG. 1. (Color online) Optical (a) and scanning electron (b) micrographs of the gold SRRs fabricated for this work. The dimensions of the SRR are approximately  $D=38 \mu\text{m}$ ,  $w=6 \mu\text{m}$ , and  $g=2 \mu\text{m}$ . The unit cell length is 50  $\mu\text{m}$ .

<sup>a)</sup>Electronic mail: phybaa@nus.edu.sg.

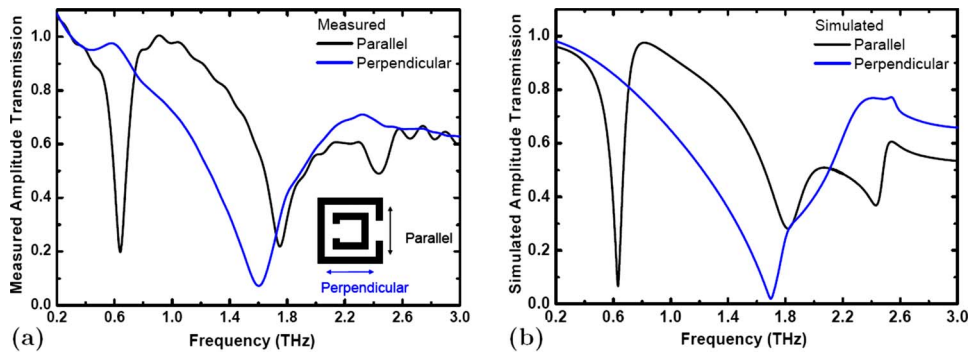


FIG. 2. (Color online) Terahertz TDS measured (a) and simulated (b) amplitude transmission. Insert in (a) shows the orientation of the SRR with respect to the electric field for the two polarizations.

cess defined SRR structures in gold, with the patterned PMMA serving as an electroplating mold. The resist was then chemically striped and the metallic seed layers on the substrate carefully etched off. This process resulted in SRRs of  $9\ \mu\text{m}$  high with highly smooth and vertical sidewalls (see Fig. 1). The sample consisted of an array of several thousand SRRs over a  $5 \times 5\ \text{mm}^2$  area.

Sample characterization was carried out by use of a photoconductive switch-based terahertz time domain spectroscopy (TDS) system, in which four parabolic mirrors are arranged in an 8 F confocal geometry.<sup>8</sup> A Kerr-lens mode-locked Ti:sapphire laser capable of generating 26 fs and 86 MHz pulses is used as the excitation source for terahertz pulses. While this confocal configuration enables excellent beam coupling between the transmitter and the receiver, a frequency-independent 3.5-mm-diameter terahertz beam waist is achieved. The beam thus covers an area containing several thousands of SRRs. The terahertz TDS system has a useful bandwidth of 0.1 to 4.5 THz and signal-to-noise ratio (S/N) of 80 dB. In order to further increase S/N, each curve is an average of six individual measurements.

Simulations were performed using the commercially available software, MICROWAVE STUDIO<sup>TM</sup> from Computer Simulation Technologies. These were carried out for a single unit cell in time domain. The simulation domain had perfect electrical and perfect magnetic conductor boundary conditions for the sides and open boundary conditions for the ends. We modeled gold as a lossy metal with conductivity  $=4.09 \times 10^7\ \text{Sm}^{-1}$ . The electrical permittivity of the silicon substrate is taken to be 11.6 (Ref. 9) with tangent  $\delta=4 \times 10^{-3}$ .

Figure 2 shows the transmission spectra of our sample. Measurements were made with the sample plane normal to the beam for two orthogonal polarizations of the electric field. When the electric field is parallel to the gap side of the SRR, there is a prominent dip in the transmission at approximately 0.64 THz [black curve in Fig. 2(a)]. This dip is absent

if the electric field polarization is rotated  $90^\circ$  (blue curve). We were able to reproduce these results with our simulations [Fig. 2(b)]. At 1.5 THz, there is another transmission dip which is present under both polarizations (though slightly redshifted under parallel polarization).

The transmission dip at 0.64 THz under parallel polarization is attributed to an inductor-capacitor (LC) resonance of the outer ring. At this frequency, simulations show circular currents in the outer ring with capacitive charge accumulation at the gaps. A SRR can be modeled as a LC circuit element with a resonance at frequency  $\omega_{LC} \propto (LC)^{-1/2}$ .<sup>10</sup> Incident electromagnetic radiation can couple to this resonance. Under our experimental geometry with the beam perpendicular to the sample plane, the LC resonance is excited only under parallel polarization.<sup>11,12</sup> The broader dip at about 1.5 THz is attributed to an electrical dipole resonance of the outer ring due to antennalike couplings between the SRRs and the incident electric field.

For this work, we shall focus on the sharper LC resonance at  $\sim 0.64$  THz and study its frequency shift with a dielectric overlayer. In Fig. 3, we show how the measured spectra changes as layers of photoresist (Futurrex Inc.,  $\epsilon=2.7 \pm 0.2$  at 1.0 THz) are spin coated onto the sample. We see that  $\Delta\omega$  increases as more layers of photoresist are added. By the third layer, the photoresist completely covered the SRRs and it appears that the frequency shift is beginning to saturate. The resonance frequency has shifted in about 0.52 THz, a shift in almost 120 GHz or 18%. The spincoating speed was set to yield a  $4\ \mu\text{m}$  thick layer. However, microscopic observation indicated that the first layer was considerably thicker than  $4\ \mu\text{m}$ , as the resist flow was obstructed by the  $9\ \mu\text{m}$  high SRR array. We estimate the final thickness to be about 16–17  $\mu\text{m}$ , with the first layer 8–9  $\mu\text{m}$  thick. Simulated data matched experimental results well.

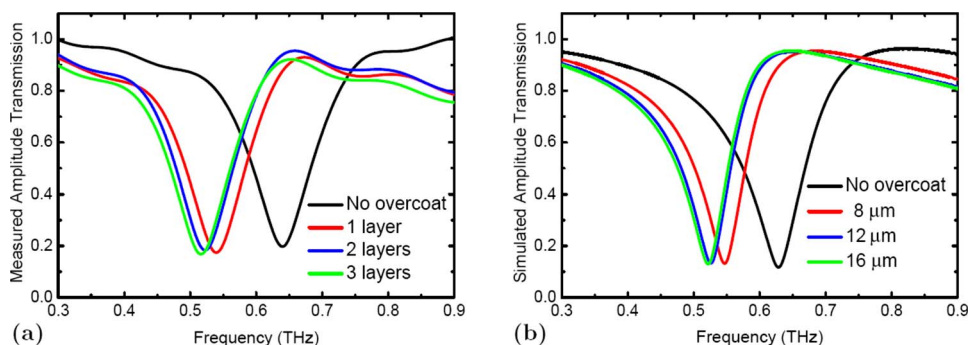


FIG. 3. (Color online) Terahertz TDS measured (a) and simulated (b) amplitude transmission as layers of photoresist with  $\epsilon=2.7$  are added.

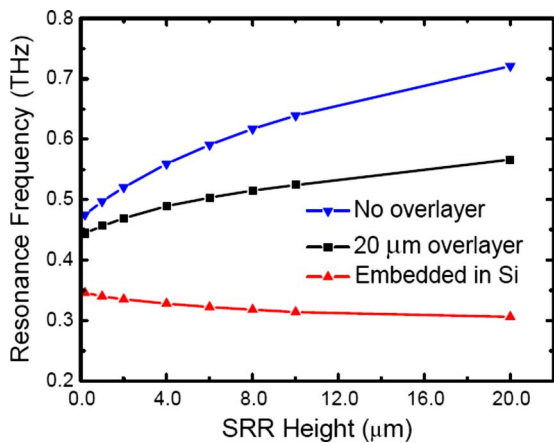


FIG. 4. (Color online) Plot of simulated  $\omega_{LC}$  for SRRs without (blue curve) and with (black curve) a 20  $\mu\text{m}$  dielectric overlayer. For SRRs, completely embedded in Si (red curve), the trend is reversed.

A suitable comparison for this present work is that of O'Hara *et al.*,<sup>1</sup> where the dimensions of the SRRs are similar but the height is about 200 nm. The SRRs were fabricated on a Si substrate and had  $\omega_{LC}=0.460$  THz. Using the same resist as this present work, O'Hara *et al.*<sup>1</sup> reported a maximum  $\Delta\omega$  of 30 GHz (about 7%) when less than 20  $\mu\text{m}$  of resist is applied. This indicates that increased aspect ratio leads to a larger maximum frequency shift. Additional evidence for the benefit of increased aspect ratio is presented in Fig. 4. Here, we show the simulated  $\omega_{LC}$  for SRRs of varying heights, with (blue curve) and without (black curve) a 20  $\mu\text{m}$  thick dielectric overlayer ( $\epsilon=2.7$ ). The substrate is Si. We see that the frequency gap between the black and blue curves increases with SRR height. Both curves show an increasing trend for  $\omega_{LC}$  but at different rates.  $\omega_{LC}$  increases faster for uncoated SRRs and thus widens the frequency gap at greater SRR heights. The difference in the rates of increase is thus important and of some interest. We carried out additional simulations to investigate the trends further.

The trend of  $\omega_{LC}$  increasing in height has also been experimentally observed in the near infrared regime by Guo *et al.*<sup>13</sup> with single split rings on a dielectric substrate. However, there are situations when this trend is reversed. Figure 4 also shows the simulated  $\omega_{LC}$  for SRRs embedded in Si (red curve). In this case,  $\omega_{LC}$  decreases as SRR height is increased. We found that changing the embedding dielectric shifts each resonance according to the relation  $\omega_{LC} \propto 1/\sqrt{\epsilon}$  but does not change the decreasing trend. In embedded SRRs, the same dielectric is present both above and below the SRR and fills the SRR gaps. The SRRs are thus under the influence of a single dielectric. Therefore, the observed decreasing trend for  $\omega_{LC}$  must be due purely to aspect ratio effects. On the other hand, SRRs attached to a dielectric substrate sit at an air-dielectric interface. In this case, the influence of the dielectric substrate diminishes with increasing SRR height—the contribution of the air filled gap will be more dominant as height increases. Therefore, the trend for

$\omega_{LC}$  is complicated by this additional effect and is expected to be different.

SRRs coated with a dielectric coating can be treated as an intermediate situation between the attached and embedded ones. In this work,  $\epsilon$  for coating is greater than in air but less than for Si. This coating replaces the air in the SRR gaps and covers the SRRs. In Fig. 4, we see that the  $\omega_{LC}$  curve for the coated SRRs (black) lies between the uncoated (blue) and embedded (red) curves. The trend is also intermediate— $\omega_{LC}$  rises with SRR height but less quickly than for the uncoated case. The slopes of the black and blue curves are thus different. This difference increases the gap between the two curves as SRR height increases.

In conclusion, we have demonstrated experimentally and numerically that high aspect ratio SRRs are able to achieve a larger frequency shift upon the application of a dielectric layer. The enhanced frequency shift would offer higher sensitivity or allow passive frequency tuning over a wider range. Thus, high aspect ratio metamaterials represent a possible option for enhancing the performance of practical devices. For this work, we have used PBW, a direct write technique valuable for fast prototyping and fundamental studies. To increase throughput for practical applications, we can use masked fabrication with, for example, a uniform broad proton beam.

The work was funded partially by the National University of Singapore grant (Grant No. NUS R144 000 204 646), the U.S. National Science Foundation, the China Scholarship Council, and the National Basic Research Program of China (Grant Nos. 2007CB310403 and 2007CB310408). We thank Dr. Abul K. Azad for useful discussions. Dr. Chammika N.B. Udalagama helped with the fabrication process. We also received technical support from Dr. Linus Lau of Computer Simulation Technologies.

<sup>1</sup>J. F. O'Hara, R. Singh, I. Brener, E. Smirnova, J. Han, A. J. Taylor, and W. L. Zhang, *Opt. Express* **16**, 1786 (2008).

<sup>2</sup>C. Debus and P. H. Bolivar, *Appl. Phys. Lett.* **91**, 184102 (2007).

<sup>3</sup>I. A. I. Al-Naib, C. Jansen, and M. Koch, *Appl. Phys. Lett.* **93**, 083507 (2008).

<sup>4</sup>T. Driscoll, G. O. Andreev, D. N. Basov, S. Palit, S. Y. Cho, N. M. Jokerst, and D. R. Smith, *Appl. Phys. Lett.* **91**, 062511 (2007).

<sup>5</sup>H. T. Chen, J. F. O'Hara, A. K. Azad, A. J. Taylor, R. D. Averitt, D. B. Shrekenhamer, and W. J. Padilla, *Nat. Photonics* **2**, 295 (2008).

<sup>6</sup>F. Watt, M. B. H. Breese, A. A. Bettiol, and J. A. van Kan, *Mater. Today* **10**, 20 (2007).

<sup>7</sup>J. A. Van Kan, A. A. Bettiol, K. Ansari, E. J. Teo, T. C. Sum, and F. Watt, *Int. J. Nanotechnol.* **1**, 464 (2004).

<sup>8</sup>M. He, A. K. Azad, S. Ye, and W. Zhang, *Opt. Commun.* **259**, 389 (2006).

<sup>9</sup>D. Grischkowsky, S. Keiding, M. van Exter, and C. Fattinger, *J. Opt. Soc. Am. B* **7**, 2066 (1990).

<sup>10</sup>S. Linden, C. Enkrich, M. Wegener, J. F. Zhou, T. Koschny, and C. M. Soukoulis, *Science* **306**, 1351 (2004).

<sup>11</sup>P. Gay-Balmaz and O. J. F. Martin, *J. Appl. Phys.* **92**, 2929 (2002).

<sup>12</sup>N. Katsarakis, T. Koschny, M. Kafesaki, E. N. Economou, and C. M. Soukoulis, *Appl. Phys. Lett.* **84**, 2943 (2004).

<sup>13</sup>H. C. Guo, N. Liu, L. W. Fu, H. Schweizer, S. Kaiser, and H. Giessen, *Phys. Status Solidi B* **244**, 1256 (2007).